CHEMISTRY
A EUROPEAN JOURNAL

DOI: 10.1002/chem.200500718

Innocent and Less-Innocent Solvent Ligands: A Systematic Investigation of Cationic Iron Chloride/Alcohol Complexes by Electrospray Ionization Mass Spectrometry Complemented by DFT Calculations

Claudia Trage,[a] Martin Diefenbach,[b] Detlef Schröder,*[a] and Helmut Schwarz*[a]

Dedicated to Professor Bernd Giese on the occasion of his 65th birthday

Abstract: The influence of anionic and neutral ligands on the reactivity of cationic iron complexes towards methanol, ethanol, and iso- and *n*-propanol has been investigated by means of electrospray ionization (ESI) mass spectrometry, and in key questions the experimental results are supported by DFT calculations. The chemical processes taking place when $FeCl_2^+$ is coordinated to a variable number of alcohol molecules were investigated by collision experiments, as well as reactivity and labeling studies. The most abundant cations formed upon ESI of $FeCl_3$/ROH mixtures can be described as consisting of a covalently bound $FeCl_2^+$ core, which is stabilized by neutral ROH ligands, for example, $FeCl_2(CH_3OH)_n^+$. Indications for a hydrogen-bonding mechanism of ligands in the second coordination sphere are given by the observation of the formally hypercoordinated ion $FeCl_2(CH_3OH)_5^+$ and interpretation of kinetic data for $n=4$. Further, deuterium labeling experiments disclose a number of hidden hydrogen transfers and imply that complexes with $n=1$ and 2 can exist in two tautomeric forms. Upon change of the alcohol ligand from methanol to ethanol and propanol, additional reaction pathways become accessible, among which metal-assisted dehydration of the respective alcohols by means of an ion/dipole mechanism is the most important.

Keywords: hydrogen transfer · iron chloride · mass spectrometry · metal alkoxides · solvent effects

Introduction

While almost all chemical reactions in the condensed phase take place in close interaction with the immediate environment, the specific role of solvent molecules in chemical processes is often difficult to assess. In the case of bond activation by a transition-metal fragment, for example, the solvent may either act as a mere spectator ligand, be actively involved by triggering the formation of a particularly reactive (or stabilized) intermediate, mediating a proton-transfer reaction and so forth, or even lose its innocence by being subjected to bond activation itself.

Gas-phase ion chemistry—often in conjunction with theory—has considerably contributed to the understanding of intrinsic ligand effects in chemical reactions and has uncovered the operation of different types of ligand effects in solvated metal ions.[1–3] The particularly unique features of electrospray ionization (ESI)[4,5] mass spectrometry offer the option to address the topic of solvation directly.[6–9] Here, we report a systematic ESI study of the cationic complexes formed from solutions of $FeCl_3$ in alcoholic solvents.[10] $FeCl_3$ was chosen as a readily soluble salt of a redox-active metal. An alcohol as a solvent allows for various types of solvation mechanisms (mere association, solvolysis, hydrogen bonds, etc.), as well as a potential reagent for bond activation. Finally, iron(III) was chosen rather than iron(II), because solvent stabilization is expected to be more important the higher the oxidation state of the metal is, such that the role of the solvent as being innocent or not can hopefully be worked out more clearly.

---

[a] Dr. C. Trage, Dr. D. Schröder, Prof. Dr. H. Schwarz
Institut für Chemie, Technische Universität Berlin
Strasse des 17. Juni 135, 10623 Berlin (Germany)
Fax: (+49) 303-142-1102
E-mail: Detlef.Schroeder@TU-Berlin.de
Helmut.Schwarz@mail.chem.TU-Berlin.de

[b] Dr. M. Diefenbach
Center for Superfunctional Materials
Department of Chemistry
Pohang University of Science and Technology San 31
Hyojadong, Namgu Pohang 790–784 (Korea)

Results and Discussion

In general, the iron-containing cations formed upon ESI of $FeCl_3/ROH$ mixtures can be attributed to four different mononuclear cluster series, namely, $FeCl_2(ROH)_n^+$, $FeCl(OR)(ROH)_n^+$, $Fe(OR)_2(ROH)_n^+$, and $FeCl(ROH)_n^+$ with n up to 5. In addition, some binuclear metal clusters are formed upon ESI, namely, $Fe_2Cl_4(OR)(ROH)_n^+$ and $Fe_2Cl_3(OR)_2(ROH)_n^+$. In this work, we will focus on the most abundant ions, formally bearing an $FeCl_2^+$ core and being solvated by a varying number of alcohol ligands.

$FeCl_3$ in methanol: At low cone voltages, corresponding to mild ionization conditions, the higher solvated representatives of the $FeCl_2(CH_3OH)_n^+$ series are most prominent in the ESI cation spectra of iron(III) chloride in methanol. Multiply solvated complexes with $n=3$, 4 dominate the mass spectra, and even small amounts of $FeCl_2(CH_3OH)_5^+$ can be observed under mildest conditions (Figure 1). With increasing cone voltages, successive desolvation leads to complexes with a smaller number of methanol ligands, like $FeCl_2(CH_3OH)_2^+$, $FeCl_2(CH_3OH)^+$, and eventually to unsolvated $FeCl_2^+$.

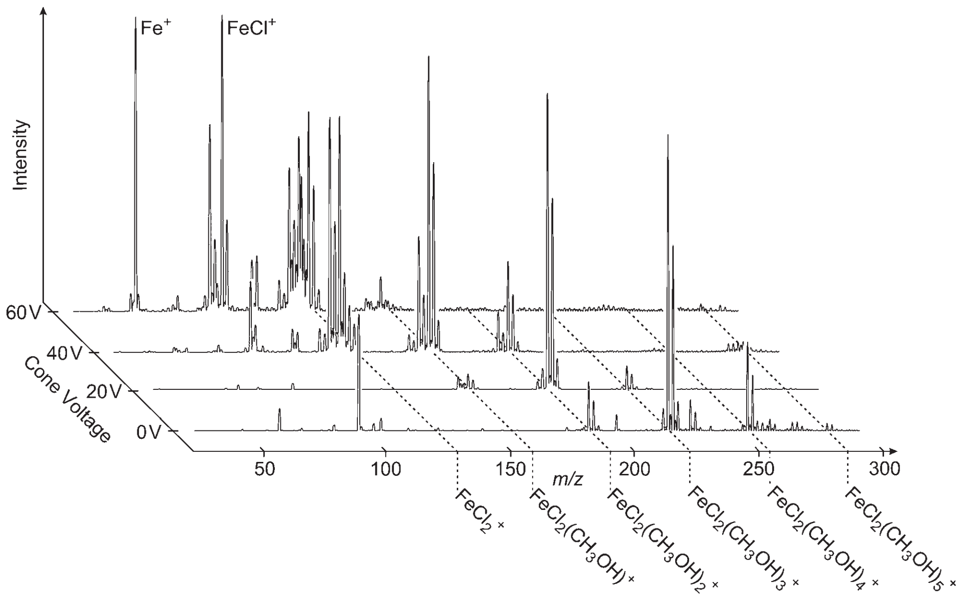

Figure 1. ESI mass spectra of solutions of $FeCl_3$ in methanol at various cone voltages.

To characterize the ion structures and bonding situations, the $FeCl_2(CH_3OH)_n^+$ complexes were investigated by means of collision-induced dissociation (CID) experiments.

The fragmentation pattern of monosolvated $FeCl_2(CH_3OH)^+$ is characterized by three exit channels. Thus, loss of the methanol ligand competes with the elimination of HCl as a low-energy process and with the expulsion of a chlorine atom; the latter is only observed at elevated collision energies (Figure 2).[11] Homolytic fission of the Fe–Cl bond, resulting in the loss of neutral Cl, lowers the partial charge on iron and formally corresponds to a reduction of the metal center to an Fe^{II} complex. By definition, the charge of bare Fe^+ is $q(Fe)=+1$, whereas the partial charge of the metal successively increases in the presence of chlorine ligands to $q(Fe)=+1.41$ in $FeCl^+$ and $q(Fe)=+1.52$ in $FeCl_2^+$.[12] Hence, Fe–Cl cleavage offers a way to stabilize the complexes by lowering the partial charge of the metal center. The latter is expected to be largest for the poorly solvated complexes, and homolytic Fe–Cl fission is, therefore, most likely to occur at a low degree of solvation, as is observed experimentally.

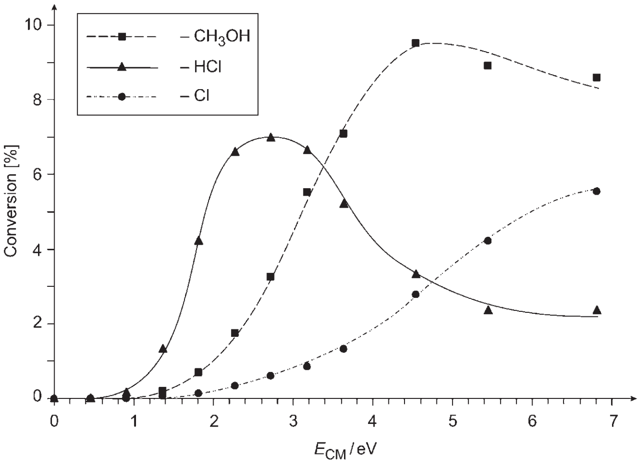

Figure 2. Breakdown graph of the CID fragments of mass-selected $FeCl_2(CH_3OH)^+$ as a function of collision energy in the center-of-mass frame.

Next, the expulsion of a HCl molecule is addressed, as it provides qualitative insight into the potential-energy surface of $FeCl_2(CH_3OH)^+$. According to Figure 2, the elimination of HCl bears a lower appearance energy than the direct loss of methanol, then shows a characteristic increase in intensity which peaks at about $E_{CM}=2.5$ eV, and finally declines at higher collision energies, at which expulsion of methanol becomes more favorable. Such an energy-behavior of the HCl loss implies that in the case of $FeCl_2(CH_3OH)^+$ the sole description of the ion in terms of an $FeCl_2^+$ core ligated by methanol is incomplete, as direct elimination of HCl is impossible from this structure; rather rearrangement to $FeCl(OCH_3)(HCl)^+$ is required prior to dissociation. In this context, knowledge of the relative energies of the two tautomers is essential. Figure 3 shows the DFT-based free-energy profile for the competing

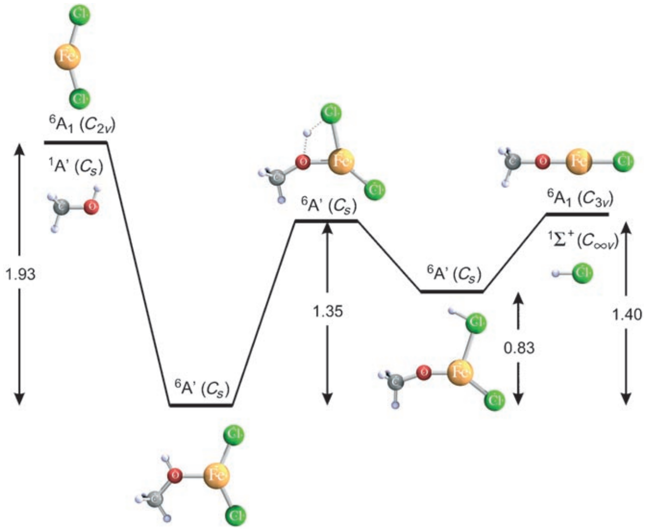

Figure 3. Free-energy profile (ΔG_{298} in eV) for the competing losses of methanol and HCl from the cationic $FeCl_2(CH_3OH)^+$ complex based on DFT calculations. See Computational Details.

losses of methanol and HCl from the cationic $FeCl_2(CH_3OH)^+$ complex. The $FeCl_2(CH_3OH)^+$ tautomer is accordingly predicted to be 0.83 eV more stable than $FeCl(OCH_3)(HCl)^+$. The corresponding transition barrier for converting one isomer into the other (1.35 eV) is located slightly below the exit channel for HCl elimination which requires 1.40 eV relative to $FeCl_2(CH_3OH)^+$. Hence, the experimentally observed losses of HCl as well as methanol from $FeCl_2(CH_3OH)^+$ are ascribed to be subject to thermodynamic control.[13] The calculated dissociation energy for the loss of methanol amounts to 1.93 eV, which is in good agreement with the experimentally obtained appearance energy AE = 1.9 ± 0.2 eV. The computationally estimated dissociation energy for the elimination of HCl of 1.40 eV is also in reasonable agreement with the experimental value of 1.2 ± 0.2 eV (see Table 1).

Table 1. Appearance energies [AE, in eV] for the indicated neutral losses upon CID of mass-selected $FeCl_2(CH_3OH)_n^+$ ions.

n	AE($-CH_3OH$)	AE($-HCl$)	AE($-Cl$)
1	1.9 ± 0.2	1.2 ± 0.2	2.4 ± 0.5
2	1.3 ± 0.2	1.0 ± 0.2	3.0 ± 0.5
3	0.4 ± 0.2		
4	0.3 ± 0.2		
5	< 0.3		

The next higher homologue, $FeCl_2(CH_3OH)_2^+$, qualitatively exhibits the same fragmentation behavior, thereby indicating a similar binding situation in which tautomerization from $FeCl_2(CH_3OH)_2^+$ to $FeCl(OCH_3)(HCl)(CH_3OH)^+$ enables the elimination of HCl as the thermodynamically most favorable exit channel. For the higher solvated complexes with $n > 2$, loss of methanol is observed exclusively (Table 1).

The appearance energies of the Cl expulsions observed for $n = 1$ and 2 are also worthy of mentioning. Although within common error limits, the larger AE observed for the more solvated cluster can be traced back to several reasons. At first, a kinetic shift might be operative in the ion dissociation process that increases the AE for the larger cluster ion, particularly because competitive kinetic shifts also come into play here.[14] In addition, the increase of the AEs can be associated with an intrinsic effect of solvation. In this respect, we refer to a related study of iron hydroxide ions.[15] Thus, the bond dissociation energy BDE(Fe^+-OH_2) = 1.3 eV is significantly smaller than BDE($HOFe^+$-OH_2) = 2.3 eV and a corresponding Born–Haber cycle implies that BDE(H_2OFe^+-OH) = 4.8 eV exceeds BDE(Fe^+-OH) = 3.8 eV by the same amount. Hence, we conclude that solvation of the metal cation also increases the bond energies to covalent ligands as indicated by the increased AEs associated with the loss of Cl. This phenomenon can be rationalized by considering the increase of the partial charge of the metal atom induced by a covalent, electronegative ligand, such as Cl or OH. Solvation by a σ-donor compensates the increased partial charge and thereby stabilizes higher oxidation states.

To corroborate the findings for the ions of the $FeCl_2(CH_3OH)_n^+$ series, their reactions with methanol are described next. Bare $FeCl_2^+$ reacts most efficiently with CH_3OH, and the reaction channel corresponds to a formal exchange of a chloro by a methoxo ligand (Table 2). This finding is in pleasing agreement with the CID experiments of mass-selected $FeCl_2(CH_3OH)^+$, which indicated the possibility of hydrogen migration to form the tautomer $FeCl(OCH_3)(HCl)^+$. The next higher homologue in the $FeCl_2(CH_3OH)_n^+$ series, that is, $n = 1$, represents the second most reactive ion. With $k_{rel} = 24 \pm 2\,\%$ it shows exchange of HCl with methanol as well as some amount of adduct formation. Again, observation of the former reaction is in good agreement with the CID results. The reaction mechanism is expected to follow an analogous route as depicted for bare $FeCl_2^+$. Despite the fact that the second reaction channel, that is, adduct formation, corresponds to the energetically more desirable increase of solvation of the complex, under the experimental conditions chosen this process is disfavored by about a factor of ten in comparison to the ligand-exchange reaction. This behavior can be ascribed to the difficulty to dissipate the internal energy that is released in the encounter complex upon coordination and either requires a

Table 2. Relative rates[a] k_{rel} and branching ratios for the reaction of $FeCl_2(CH_3OH)_n^+$ with CH_3OH.[b]

n	k_{rel} [%]	$+CH_3OH/-HCl$	$+CH_3OH$
0	37 ± 4	100	
1	24 ± 2	91 ± 2	9 ± 2
2	0.04 ± 0.01		100

[a] The fastest reaction investigated ($FeCl_2(CH_3OH)_5^+ + CD_3OD$, Table 3) serves as reference for the relative rates reported here. [b] For $n > 2$, ligand loss has been observed exclusively.

collision with a third body or deactivation through radiative transition.[16] Under the pressure conditions that prevail in the present experiments, the lifetime of the encounter complex is, hence, ascribed to play an important role, as deactivation is more likely to occur prior to dissociation if the complex is long-lived.

In case of $n=2$, adduct formation constitutes the sole reaction channel observed, but its very low efficiency is expressed in the small relative rate of $k_{rel}=0.04\pm0.01\,\%$. The substantial drop in reactivity can be ascribed to the result of two opposing trends in adduct formation. While a larger molecular size should kinetically enhance the lifetime of the encounter complex, the thermodynamic driving force associated with binding another molecule diminishes with increasing solvation. Further, the absence of the respective exchange of HCl by CH_3OH in case of $n=2$ suggests that $FeCl_2(CH_3OH)_2^+$ does not coexist with its tautomer in the ion beam prior to collision; rather collisional activation is indeed mandatory to initiate tautomerization. As already implied from the CID experiments, no tautomerizations take place for $n=3$, and hence no exchange of HCl by methanol can be observed in the reaction of $FeCl_2(CH_3OH)_n^+$ with methanol for $n=2$. Accordingly, the higher homologues show neither exchange of HCl nor adduct formation in their reactions with methanol, but only increasing amounts of fragmentation at low collision energy.

To investigate the reactivity of the $FeCl_2(CH_3OH)_n^+$ complexes with respect to degenerate ligand exchange and to reveal possible hidden hydrogen migrations, analogous experiments were performed with CD_3OD present in the hexapole collision cell instead of CH_3OH. Relative reaction rates were determined by correlating the reactivities with the most reactive ion investigated, that is, $FeCl_2(CH_3OH)_5^+$.

Consistent with the results obtained for CH_3OH, the reaction of $FeCl_2^+$ with CD_3OD shows the exchange of a chloro by a CD_3O ligand and concomitant elimination of DCl (Table 3). In marked contrast to the non-deuterated case, $n=0$ represents the least reactive ion of this series. For $n=1$, the reaction products comprise exchange of CH_3OH by CD_3OD ($\Delta m=+4$), exchange of $H^{37}Cl$ as well as $D^{37}Cl$ by CD_3OD ($\Delta m=-2$, -3), and adduct formation ($\Delta m=+36$). These four channels are expected for the reaction of $FeCl_2(CH_3OH)^+$ and its tautomer with CD_3OD, but yet comprise only 82 % of all products. In addition, mass shifts of $\Delta m=+3$ and $+1$ are observed, the origin of which is explained in Scheme 1.

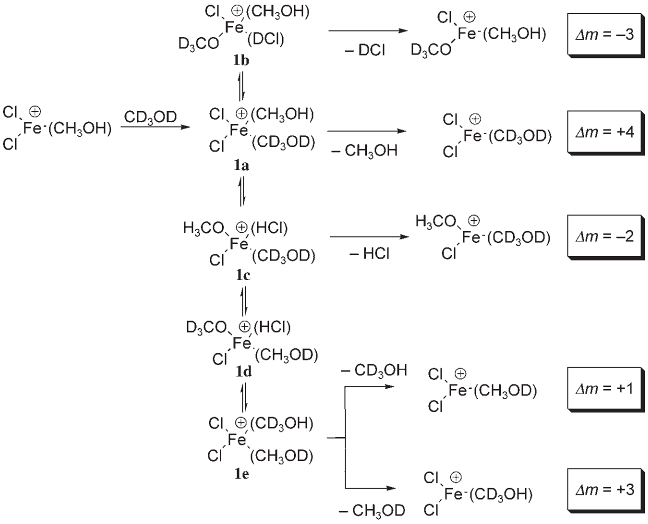

Scheme 1. Simplified isomerization sequence for reaction of $FeCl_2(CH_3OH)^+$ with CD_3OD; note that each separate transformation may further consist of several steps. For example, the interconversion of **1c** into **1d** may proceed through intermediate migration of the deuterium atom to chlorine.

In the reaction of $FeCl_2(CH_3OH)^+$ and CD_3OD, the encounter complex **1a** is formed initially, which can either directly lose the CH_3OH ligand, resulting in $\Delta m=+4$, or expel CD_3OD corresponding to the reverse reaction with $\Delta m=0$. However, sufficient energy is liberated upon formation of **1a** to enable tautomerizations to either **1b** or **1c** prior to dissociation. These rearranged complexes are expected to lose DCl and HCl, respectively, which in turn account for the signals at $\Delta m=-3$ and -2. The eliminations of CD_3OH ($\Delta m=+1$) and CH_3OD ($\Delta m=+3$) require further tautomerization up to **1e**.[17] Several of these channels are therefore expected to be sensitive towards a variation of the lifetime of the encounter complex, as they require repeated passages through the isomerization processes prior to fragmentation. In some additional experiments, the lifetime of the proposed encounter complex $Fe^{37}Cl_2(CH_3OH)(CD_3OD)^+$ was varied by changing the collision energy from $E_{CM}=0$ eV to $E_{CM}=0.6$ eV.[18] All reaction channels requiring hydrogen rearrangements prior to ligand loss were strongly affected by shortening the lifetime of the encounter complexes, fully consistent with a diminished probability of rearrangements. The fact that the exchange of $H^{37}Cl$ with CD_3OD ($\Delta m=-2$) is also strongly lifetime-dependent, further corroborates the claim that no tautomerization of $FeCl_2(CH_3OH)^+$ takes place prior to collision; otherwise, any preformed HCl ligand should easily exchange with CD_3OD, even at shorter lifetimes.

The reactions of the multiply solvated ions, $FeCl_2(CH_3OH)_n^+$ ($n=2$–5), with CD_3OD are consistent with the findings for

Table 3. Relative rates and branching ratios for the reactions of mass-selected $FeCl_2(CH_3OH)_n^+$ with CD_3OD.

n	k_{rel} [%]	$\Delta m=+4$ $+CD_3OD$-CH_3OH	$\Delta m=+3$ $+CD_3OD$-CH_3OD	$\Delta m=+1$ $+CD_3OD$-CD_3OH	$\Delta m=-2$ $+CD_3OD$-HCl	$\Delta m=-3$ $+CD_3OD$-DCl	$\Delta m=+36$ $+CD_3OD$
0	37±4					100	
1	89±9	23±3	7±3	11±1	28±1	23±1	8±1
2	70±7	100					
3	85±8	100					
4	96±9	100					
5	100	100					

CH_3OH, and the resulting reaction patterns simplify markedly for $n=2$ in that they are restricted to an exchange of CH_3OH by CD_3OD. No tautomerization enabling the liberation of HCl or DCl is observed for $n=2$. A comparison of the relative rates for the reaction with non-deuterated and deuterated methanol shows opposing trends with molecular size. While the reactivity in the reaction with CH_3OH is rapidly declining with size, the opposite holds true for CD_3OD. The main difference between the two experiments concerns the observation of degenerate ligand exchange in one case, whereas the same remains undetected in the other. As shown in Figure 4, ligand exchange takes place increasingly faster with growing number of ligands n; this fact can be understood by consideration of statistical as well as intrinsic effects. As indicated by the dashed line in Figure 4, the qualitative general trend of increasing reactivity can by and large be rationalized in terms of statistical arguments.[19] According to Equation (1), the probability of a successful exchange, that is, that the leaving methanol ligand is non-deuterated, increases with the number of non-deuterated methanol ligands initially present in the molecule, as reflected in the probability of exchange (p_{exch}), which rises from 50 % for $n=1$ to 83 % for $n=5$.

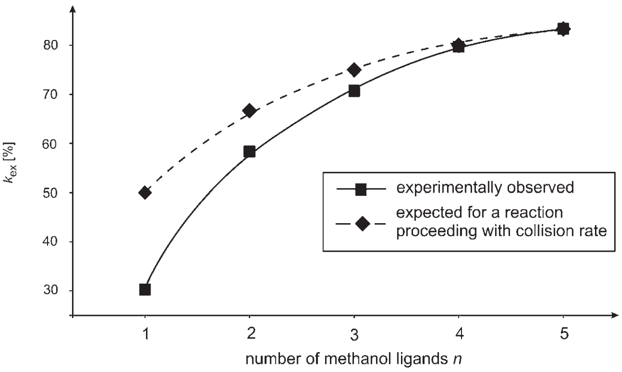

Figure 4. Experimentally observed rates k_{ex} for the degenerate methanol exchange in dependence of the number of neutral ligands n and the expected trend if ligand exchange takes place with collision rate.

$$\mathrm{FeL}_n^+ + \mathrm{L}' \rightleftharpoons [\mathrm{FeL}_n\mathrm{L}'^+] \rightleftharpoons \mathrm{FeL}_{n-1}\mathrm{L}'^+ + \mathrm{L} \qquad p_{\mathrm{exch}} = \frac{n}{n+1} \tag{1}$$

The dashed line in Figure 4 accordingly represents the reactivity trend expected for ligand exchange occurring with collision rate. While these considerations provide a qualitative explanation for the observed trends, intrinsic effects must play an additional role in order to explain the remaining differences. Specifically, all experimentally observed rates fall short of the values expected for a reaction proceeding with collision rate, and the differences decrease with increasing number of methanol ligands. For the sake of simplicity, let us assume in the following that the reaction does take place with collision rate. In this case the experimental rate k_{ex} should coincide with the statistically determined rate k_{stat} [Eq. (2)]. The related exchange rates for the remaining $FeCl_2(CH_3OH)_n^+$ ($n=1$–4) ions can then be characterized by introducing a factor x, which expresses the fraction of how much the experimental rates deviate from purely collision-controlled processes [Eq. (3), Table 4].[20]

$$k_{\mathrm{ex}}(\mathrm{FeCl_2(CH_3OH)_5^+}) \mathrel{\hat{=}} k_{\mathrm{stat}}(\mathrm{FeCl_2(CH_3OH)_5^+}) \tag{2}$$

$$k_{\mathrm{ex}}(\mathrm{FeCl_2(CH_3OH)}_n^+) = x\, k_{\mathrm{stat}}(\mathrm{FeCl_2(CH_3OH)}_n^+) \tag{3}$$

Table 4. Deviation from collision-controlled reaction (x) in dependence of n.

n	1	2	3	4	5
x	0.61	0.88	0.94	0.99	1.00
x'[a]	0.74	0.82	0.88	0.94	1.00

[a] The parameter x' includes an estimated correction for the different ion masses, assuming a small, but finite velocity of the ions at a collision energy nominally set to 0 eV. Despite some numerical difference, the qualitative conclusions are the same. A more precise quantification for $E_{\mathrm{lab}}=0$ eV is impossible in the experimental set-up used (also see Experimental Section).

Evidently, the intrinsic effects that lead to increasing exchange rates for larger complexes cannot be of energetic nature as we are dealing with a degenerate reaction.[21] Hence, kinetic reasons are to be considered instead. Assuming a single-minimum potential-energy diagram for the exchange reaction (Figure 5a) is insufficient for the description of the case at hand, because a single minimum with degenerate exit channels solely reflects the statistical effects and is accordingly expected to proceed with collision rate.

Consequently, ligand exchange must proceed through a multistep mechanism including at least one reaction barrier that induces a kinetic hindrance in order to provide an explanation as to why the reaction rate falls short of the collision rate (Figure 5b).

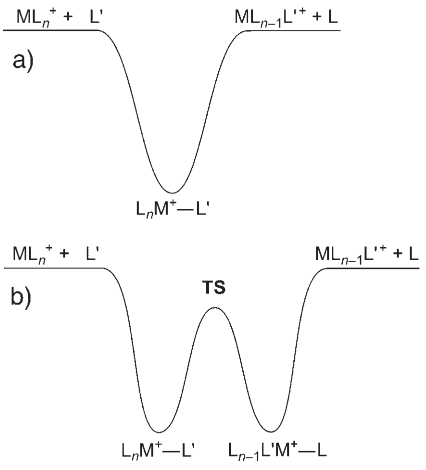

Figure 5. Suggested single- and double-minimum paths for the ligand exchange of L = CH_3OH by L′ = CD_3OD (M = $FeCl_2$).

Having deduced the existence of a reaction barrier for the CH_3OH/CD_3OD exchange, an elucidation of the connected chemical origin is warranted. A valuable hint is given by the $FeCl_2(CH_3OH)_5^+$ ion, the mere existence of which is ascribed to external hydrogen bonding between the first solvation sphere of four methanol and two chloro ligands and the fifth CH_3OH molecule as mentioned above. Accordingly, it seems likely that an incoming methanol molecule—here CD_3OD—is initially coordinated loosely through external hydrogen bonding to the already present methanol ligands before reorganization takes place (Scheme 2). Finally, a successful CH_3OH/CD_3OD exchange will pass through a comparable encounter complex in which the ligand-to-leave is now coordinated through hydrogen bonds prior to final dissociation.

Scheme 2. Schematic representation for degenerate ligand exchange in the octahedral complex $FeCl_2(CH_3OH)_4^+$ via an encounter complex in which the incoming CD_3OD ligand is attached by means of hydrogen bonding.

$FeCl_3$ in ethanol: To investigate the influence of the alcohol, ROH, on the ions formed, methanol was replaced systematically by ethanol, *n*-propanol, isopropanol, and *tert*-butanol. As far as the ions formed upon ESI of solutions of $FeCl_3$ in ROH are concerned, the qualitative picture by and large remains unchanged if R varies from CH_3 to C_2H_5. $FeCl_2(ROH)_n^+$ ($n=0$–4) complexes are observed as well as $FeCl(OR)(ROH)_n^+$ ($n=1$, 2) and $FeCl(ROH)_n^+$ ($n=0$–3).

However, pronounced differences occur upon CID of the monosolvated cation $FeCl_2(ROH)^+$ (Table 5). Instead of the HCl loss observed for $R=CH_3$, elimination of C_2H_4 takes place in case of $R=C_2H_5$. This process corresponds to a metal-assisted cleavage of C_2H_5OH to water and ethene, which is impossible for $R=CH_3$. With an appearance energy as low as $AE=0.7\pm0.1$ eV, ethene elimination constitutes the lowest-energy pathway for the dissociation of $FeCl_2(C_2H_5OH)^+$. Interestingly, even a single additional ligand suffices to completely suppress this type of bond-activation process, as shown by the absence of ethene elimination from $FeCl_2(C_2H_5OH)_n^+$ with $n=2$.

Table 5. Appearance energies [AE, in eV] for the indicated neutral losses upon CID of mass-selected $FeCl_2(C_2H_5OH)_n^+$ ions.

n	AE($-C_2H_5OH$)	AE($-HCl$)	AE($-Cl$)	AE($-C_2H_4$)
1	2.0 ± 0.2		3.0 ± 0.5	0.7 ± 0.1
2	1.1 ± 0.2	0.8 ± 0.1		
3	0.2 ± 0.2			
4	< 0.2			

In the context of dehydration and dehydrohalogenation of alcohols and alkylhalides mediated transition-metal cations, two different mechanisms have been suggested in the literature.[22–24] While in some cases, evidence exists for an insertion of the metal into the C−X bond (X = OH, Hal) followed by a β-hydrogen shift, other systems are better described in terms of the so-called ion–dipole mechanism in which the metal cation first coordinates to X and invokes a charge transfer to the alkyl backbone and then experiences a proton transfer (Scheme 3).

In the case at hand, the oxidative addition of $FeCl_2^+$ into the C−O bond of an alcohol would lead to an insertion species R-[$FeCl_2^+$]-OH with a formal iron(v) ion, the involvement of which appears rather unlikely. Bond activation by means of the ion–dipole mechanism is much more plausible. Accordingly, the $FeCl_2^+$ moiety is assumed to initially coordinate to the lone pair of the ROH oxygen followed by a (at least partial) charge transfer from the metal to the alkyl backbone. This process formally leads to an alkyl cation that is coordinated through oxygen to a neutral Cl_2FeOH entity. Proton transfer from the alkyl cation, acting as a Brønsted acid, to the hydroxyl group then generates ethene and $Cl_2Fe(H_2O)^+$ and thus completes the reaction mechanism without involving any change of the metal's oxidation state throughout the entire sequence.

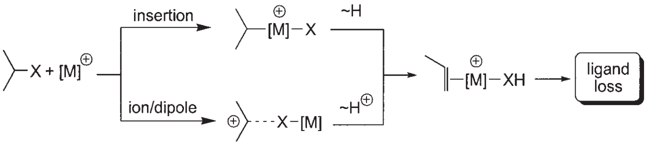

Scheme 3. Oxidative insertion and ion–dipole mechanism suggested for the metal-cation-mediated elimination of HX from alcohols and alkylhalides with X = OH and Hal, respectively.

To support this interpretation of the CID results, the reactions of the $FeCl_2(C_2H_5OH)_n^+$ with ethanol have been investigated as well (Table 6). In accordance with the CID experiments, bond activation occurs for $n=0$ and 1. The higher solvated ions ($n=2$–4) are basically nonreactive and only

Table 6. Relative rates and branching ratios for the reactions of $FeCl_2(C_2H_5OH)_n^+$ with C_2H_5OH.[a]

n	k_{rel} [%]	$\Delta m=+10$ $+C_2H_5OH$-HCl	$\Delta m=+18$ $+C_2H_5OH$-C_2H_4	$\Delta m=+28$ $+C_2H_5OH$-H_2O	$\Delta m=+46$ $+C_2H_5OH$
0	100	11 ± 1	60 ± 6	6.0 ± 0.6	23 ± 2
1	61 ± 6	67 ± 7	1.4 ± 0.1		32 ± 2
2	0.3 ± 0.1				100
3	0.6 ± 0.1				100

[a] For $n=4$, ligand loss is observed exclusively.

show a decreasing tendency of adduct formation with increasing *n*. Bare $FeCl_2^+$ reacts most efficiently with ethanol and hence serves as a reference for the other ions as summarized in Table 6. In addition to the elimination of HCl, which constituted the only channel observed for $FeCl_2^+$ with methanol, three further reactions take place with ethanol as a reactant, that is, eliminations of ethene and water as well as small amounts of adduct formation. The losses of ethene and water are the reaction channels corresponding to activation of the C–O bond by an ion–dipole mechanism. In order to understand why both ligand losses are observed in case of the reaction with ethanol, whereas the CID spectra showed exclusive loss of ethene, a closer look at the tetracoordinate intermediate $FeCl_2(H_2O)(C_2H_4)^+$ is enlightening (Scheme 4).

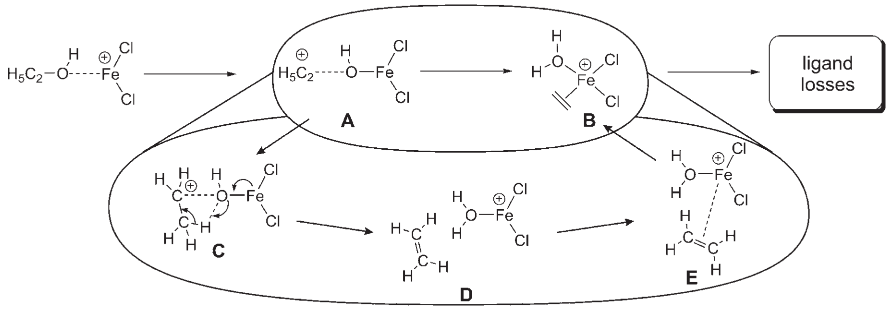

Scheme 4. Mechanistic suggestion for the formation of the tetracoordinate $FeCl_2(H_2O)(C_2H_4)^+$ complex.

Hydrogen transfer from the alkyl entity in **A** to the hydroxyl group leads to structure **B** with water and ethene acting as closed-shell ligands. However, due to the suggested mechanism of C–O bond activation, the bond between iron and oxygen is inherently present in structure **A**, while the alkene ligand generated en route to **B** is formed initially in spatial distance from the metal center. Directly after the hydrogen shift (**A**→**C**→**D**), the transient complexes are, therefore, probably better described as loosely bound ion–dipole complexes **D** and **E**. Formation of the tetracoordinate complex **B** needs a geometrical reordering to allow the ethene ligand to approach the metal center, such that the expected σ-bonding/π-back-bonding situation (Dewar–Chatt–Duncanson model)[25,26] can be established. Hence, the formation of **B** strongly depends on the lifetime of the complex. If the complex does not have sufficient time to reorganize its geometry en route to **B**, the ethene ligand is easily lost. As CID experiments deal with higher collision energies than reactivity investigations in which E_{CM} is nominally set to zero, the former shows exclusive loss of ethene, whereas evaporation of both ethene and water can compete in the latter because here the lifetime of the encounter complex is apparently long enough to allow bond formation between iron and ethene.

The reaction pattern of monosolvated $FeCl_2(C_2H_5OH)^+$ is similar to that of bare $FeCl_2^+$. For $n=1$, however, C–O bond activation decreases in favor of O–H bond activation concomitant with HCl loss such that ethene elimination represents only a minor reaction channel; the complementary expulsion of water cannot be observed, because the signal does not exceed the noise level.

Some further useful information about the reaction mechanism can be gained upon isotopic labeling. If mass-selected $FeCl_2^+$ is treated with CH_3CD_2OH in the hexapole collision cell, reactions analogous to those for the unlabeled compound are observed (Table 6), but the product patterns reveal the occurrence of H/D scrambling in the course of the reaction. Thus, the expulsion of ethene splits up into losses of $C_2H_2D_2$ and C_2H_3D (branching: 75:25), of which the former product is expected in terms of a selective 1,2-elimination. Rather than involving a putative 1,1-elimination,[27] scrambling of the labeling appears as the most plausible explanation.[28] Likewise, H/D equilibration is observed upon CID of mass-selected $FeCl_2(CH_3CD_2OH)^+$, although its extent is somewhat reduced in that the branching ratio of $C_2H_2D_2$ and C_2H_3D amounts to 85:15. The occurrence of at least partial H/D equilibration in the course of the bond-activation processes can best be understood by means of facile Wagner–Meerwein rearrangements within the intermediates (e.g., structure **A** in Scheme 4). In this context, the larger amount of H/D equilibration upon reacting mass-selected $FeCl_2^+$ with CH_3CD_2OH with respect to the CID measurement of $FeCl_2(CH_3CD_2OH)^+$ can be understood by the larger entrance energy of the former system. In fact, with regard to the ionization energy $IE(C_2H_5OH)=10.47$ eV of ethanol, $IE(FeCl_2)=10.29$ eV[29] is almost large enough to allow for a direct electron-transfer mechanism,[30] which is assisted further by generating a strong, covalent Fe–O bond in **C**.

$FeCl_3$ in propanol: In the following section, the set of alcohols investigated is augmented by inclusion of *n*- and isopropanol.[10,28] The most notable difference of the $FeCl_3$/propanol system to those discussed above is that the ESI mass spectra are dominated by metal-free organic cations, such as the proton-bound dimer $(ROH)_2H^+$ and trimer $(ROH)_3H^+$. The iron-containing cluster ions of interest are up to two orders of magnitude lower in abundance. In case of isopropanol as solvent, the only iron-containing ion series observed corresponds to $FeCl_2(ROH)_n^+$ with $n=0$–3.

As mentioned, CID experiments of $FeCl_2(ROH)^+$ revealed the occurrence of an $FeCl_2^+$-assisted elimination of water from the alcohol as already described for ethanol. In case of isopropanol, this pathway outweighs the other possible dissociation channels observed for methanol and ethanol, like simple ligand loss or HCl elimination. Instead, complementary expulsion of water and propene ligands is observed from the putative intermediate $FeCl_2(H_2O)(C_3H_6)^+$.

At low collision energies, loss of propene is only slightly favored over the expulsion of water (Figure 6). With increasing collision energy, this difference becomes more pronounced and elimination of water is eventually suppressed completely.[31] Low-energy CID by and large reflects thermodynamic factors, that is, ligand binding energies, whereas the behavior at higher collision energies is increasingly determined by kinetic factors. Hence, the binding energies of water and propene to $FeCl_2^+$ seem to be of comparable size with the former being slightly larger. Additionally, the elimination of propene is favored kinetically, as can be seen by the increasing branching ratio of this channel at elevated collision energies. This finding is in pleasing agreement with structures **D** and **E** as suggested in the electron-transfer mechanism of the $FeCl_3$/ethanol system (see Scheme 4).

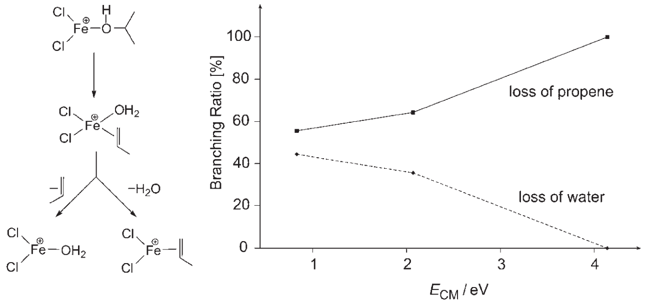

Figure 6. Energy-dependent branching ratio for the losses of water and propene upon CID of $FeCl_2(iC_3H_7OH)^+$.

The presence of a second propanol ligand, that is, $FeCl_2(ROH)_2^+$, enriches the fragmentation pattern by two additional fragmentation channels. In addition to C–O bond activation, which is concomitant with the elimination of either propene or water, O–H bond activation eventually leading to the liberation of HCl is observed. Further, loss of an intact propanol moiety is also accessible. Upon solvation with yet an additional alcohol ligand, that is, $FeCl_2(ROH)_3^+$, the CID spectrum shows exclusive expulsion of propanol.

To corroborate the results obtained with isopropanol, the corresponding complexes of $CD_3CH(OH)CH_3$ and $CD_3CH(OH)CD_3$ were also considered. Note that CID is only possible for the larger complexes, while a direct investigation of $FeCl_2(ROH)^+$ was impossible due to the extremely low abundances of these ions.[32] Within the experimental error limits, loss of propene upon CID of mass-selected $FeCl_2(CD_3CH(OH)CD_3)_2^+$ exclusively leads to C_3HD_5, rather than fully deuterated C_3D_6, which would be formed if H/D equilibration were occurring (branching ratio: $>99.4:0.6$). Hence, a selective 1,2-elimination is assumed to take place. Thus, the corresponding branching of $C_3H_4D_3$ (59%) and $C_3H_3D_2$ (41%) eliminations from $FeCl_2(CD_3CH(OH)CH_3)_2^+$ implies the operation of an intramolecular kinetic isotope effect of 1.45 ± 0.05.

With regard to the H/D equilibration in the case of ethanol as described above, it may first appear surprising that the bond activation of propanol occurs more selectively. However, this observation follows precisely the line of reasoning of the proposed operation of an ion–dipole mechanism. Thus, charge transfer and concomitant formation of a carbenium center are much more likely to occur in the fragmentation of monosolvated $FeCl_2(ROH)^+$ than for $FeCl_2(ROH)_2^+$, because the latter complex bears a higher degree of solvation of the metal center. Hence, H/D scrambling occurs for $FeCl_2(ROH)^+$, whereas it does not in $FeCl_2(ROH)_n^+$. In turn, however, it requires the more fragile isopropyl group for C–O bond activation taking place to a notable extent at all in $FeCl_2(ROH)_n^+$ complexes with $n > 1$.

Another effect is remarkable in comparing the propanol complexes. Thus, the CID spectra of $FeCl_2(ROH)_2^+$ show preferential expulsion of propene in case of ROH = isopropanol, while the losses of propanol and HCl seemingly gain in importance in case of ROH = *n*-propanol (Figure 7). The qualitatively different fragmentation behavior for $FeCl_2(ROH)_2^+$ with R = *n*- and isopropyl lends further support to the operation of an ion–dipole mechanism as suggested for the elimination of propene (and water). Thus, intermediate charge transfer from iron to the propyl moiety is energetically less favored for ROH = *n*-propanol than for isopropanol. Consequently, the amount of propene elimination decreases and fragmentation pathways that are able to circumvent a charge transfer to the *n*-propyl backbone are preferentially observed. With increasing collision energy, generation of $FeCl_2(ROH)^+$ gains in significance which can either be ascribed to a direct loss of ROH or consecutive dissociation of the primary fragments.

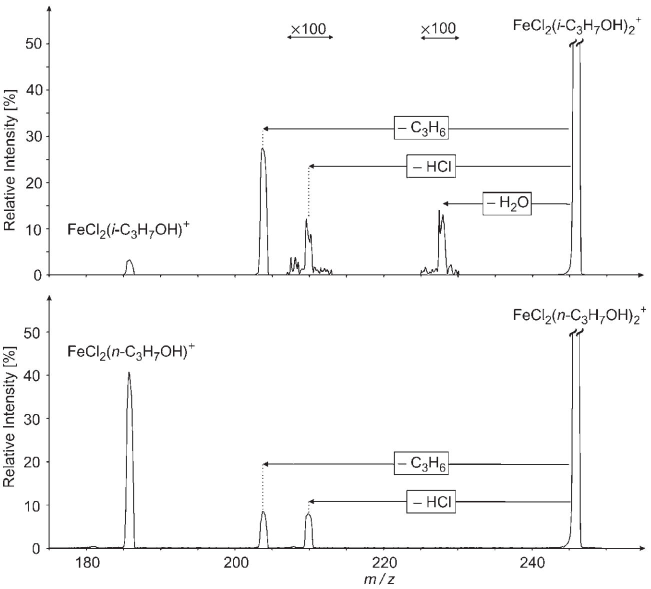

Figure 7. CID spectrum of $FeCl_2(iC_3H_7OH)_2^+$ (top) and $FeCl_2(nC_3H_7OH)_2^+$ (bottom) at $E_{lab} = 5$ eV.

In the $FeCl_3$/*n*-propanol system, the dominance of the metal-free ions is not as distinct as in case of isopropanol. Reasonable amounts of $FeCl_2(ROH)_n^+$ for $n=3$ and $n=4$ can compete with the formation of the proton-bound trimer and even surpass the proton-bound dimer at low cone voltages. The striking contrast in the behavior of *n*- and isopropanol may be attributed to the difference in proton affinity (PA) of the two isomeric alcohols. Isopropanol exhibits a larger PA (793 kJ mol^{-1}) than *n*-propanol (787 kJ mol^{-1})[33] and a similar order can be expected for the tendency of forming proton-bound dimers and trimers. As a result, the mixtures with *n*-propanol still permit the investigation of metal complexes, whereas organic ions dominate the spectra in case of isopropanol. Evidently a subtle balance in ion formation exists upon ESI of metal-salt solutions between the generation of cationized solvent molecules and metal-containing cluster cations. In this respect, the mixtures of $FeCl_3$ with *n*- and isopropanol appear to represent two borderline cases in which the relatively small difference in the proton affinities of the alcohols leads to a distinct change of the distribution between pure organic and metal-containing cations. Along this line of reasoning, it can also be understood why the investigation of the $FeCl_3$/*tert*-butanol system proved unsuccessful. Here, the even larger PA(*tert*-butanol) = 802 kJ mol^{-1}[33] leads to ESI-spectra that can be entirely ascribed to proton-bound oligomers of the alcohol.

Conclusion

The most abundant cations formed upon ESI of $FeCl_3$/ROH mixtures can be described as consisting of a covalently bound $FeCl_2^+$-core stabilized by ROH ligands, that is, $FeCl_2(ROH)_n^+$. Depending on the degree of solvation, the nature of ligation can be either described as innocent, that is, mere solvation in case of higher degrees of solvation, or the innocence of ROH as a solvent ligand is lost in the sense that processes like solvolysis, hidden hydrogen migrations, and even direct chemical processes as dehydration of the solvent ligand play a non-negligible role for lesser solvated complexes. For $n=1$ and 2, the complexes of methanol serve as an example for solvolysis as these can exist in two tautomeric forms—the energetically more stable $FeCl_2(CH_3OH)_n^+$ isomer as well as $FeCl(OCH_3)(HCl)(CH_3OH)_{n-1}^+$, which becomes energetically accessible upon collisional excitation.

Observation of the formally hypercoordinated ion $FeCl_2(CH_3OH)_5^+$ points towards a hydrogen-bonding mechanism for ligands in the second coordination sphere without direct ligation of the iron center. Deuterium labeling experiments disclose a number of hidden hydrogen transfers to be operative and further reveal that normal and redox hydrogen migrations are fast, thereby leading to an almost complete equilibration of the corresponding tautomers involved; kinetic isotope effects do not play an important role in these hydrogen migrations.

Upon change of the alcohol from methanol to ethanol and propanol, additional reaction pathways become accessible, and metal-assisted dehydration of the respective alcohols employed is observed in the lesser solvated complexes. Detailed data analysis hints towards an ion–dipole mechanism being operative.

Experimental Section

The mass spectrometric experiments were carried out on a commercial VG BIO-Q mass spectrometer which has been described in detail previously.[34] In brief, the VG BIO-Q consists of an ESI source combined with a tandem mass spectrometer of QHQ configuration (Q: quadrupole, H: hexapole). In the present experiments, millimolar solutions of anhydrous $FeCl_3$ in ROH ($R=CH_3$, C_2H_5, iC_3H_7, nC_3H_7) were introduced through a syringe pump (flow rate 10 μL min^{-1}) to the fused-silica capillary of the ESI source. Nitrogen was used as drying gas and as nebulizer gas. The source temperature was varied between 80 and 115 °C depending on the solvent composition. The cone voltages applied in the desolvation zone of the differentially pumped ESI source were systematically varied for the ions of interest (see below), which were then selected at unit mass resolution by means of Q1.

Due to natural isotope abundances, the mass spectra of $^{56}Fe^{35}L_2^+$ complexes investigated here always contained some $^{54}Fe^{35}L^{37}Cl^+$ isotopomers and hence the respective CID signals were observed. The isotope patterns of all ions described below agreed with expectation on the basis of natural isotope abundances.[35]

The cone voltage U_C determined the amount of collisional activation of the ions evolving from solution in the differential pumping system of the ESI source. At low cone voltages, multiply solvated ions were formed, which then lost the weakly bound solvent molecules at increased U_C, followed by evaporation of more strongly bound ligands including the cleavage of covalent bonds, electron-transfer processes, and so forth, and finally atomic metal cations were obtained at high cone voltages.[36] Collision-induced dissociation (CID) experiments were performed with xenon at various collision energies ($E_{lab}=0$–30 eV) and a pressure of about $3 \cdot 10^{-4}$ mbar, which approximately corresponded to single-collision conditions.[34] The collision energies were converted to the center-of-mass frame, $E_{CM}=[m/(M+m)]E_{lab}$, in which m and M are the masses of the collision gas and the ionic species, respectively. The product ions formed in the hexapole were then analyzed by scanning Q2. Further, by variation of the collision energy led to breakdown diagrams that enabled the determination of phenomenological appearance energies (AEs)[37] of the various fragmentation channels by linear extrapolation of the signal onsets to the baseline. The corresponding experimental errors were estimated by applying linear extrapolations with gradients deviating from the best possible fit, but which were still in reasonable agreement with the experimental data.

Reactivity studies were carried out by mass selection of the complex of interest with Q1, allowing it to interact with reactant in the hexapole collision cell under single-collision conditions at a collision energy nominally set to 0 eV, and mass-analysis of the reaction products by means of Q2. Relative reaction rates were determined by correlating the reactivities to that of the most reactive ion investigated. To this end, the amount of conversion of the parent was determined as $x_i=I_P/\Sigma I_i$ and inserted into $kt=-\ln(x_i)$ yielding a phenomenological expression for the relative rate of the reaction.[38,39] Further, the experimentally observed relative rates were corrected for contributions from mere fragmentation, which occurred in some cases despite a collision energy nominally set to 0 eV. As the fragmentation does not count as a reaction in a common sense, the corrected relative rates, k_{rel}, were a superior measure for the intrinsic reactivity of $FeCl_2(ROH)_n^+$ ions with ROH.

In case of $ROH=C_2H_5OH$, the reactivity investigations were superimposed by minor contributions of an unwanted side reaction for $n=1$–3. During the spray process, a certain amount of solvent always entered the mass-analyzer and may even have reached the hexapole region. For tax reasons, the ethanol employed was denatured with 2-butanone and small amounts of the admixture entered the collision cell. The presence of 2-butanone in the reaction chamber led to ligand-exchange processes as side reactions, that is, replacement of either one or two ethanol molecules by one 2-butanone ligand. All relative rates and branching ratios of the reaction of $FeCl_2(C_2H_5OH)_n^+$ with C_2H_5OH are corrected for this side reaction.[40]

To minimize unwanted H/D exchange processes with hydroxyl groups on the wall of the inlet lines and the collision cell in case of reactivity studies with CD_3OD, the collision cell was purged with [D$_4$]methanol twice for 30 minutes prior to the actual experiments.

Computational details: Density functional calculations were performed by using the *m*PW1PW91[41] hybrid functional in conjunction with the standard triple-zeta type basis sets 6–311+G(d,p), as implemented in Gaussian 03.[42] On iron, the ten 1s2s2p core electrons were replaced by the Stuttgart–Dresden–Bonn (MDF type) scalar relativistic pseudopotential;[43] for the valence space, the corresponding (8s7p6d1f)/[6s5p3d1f] basis set was employed. Local minima and transition structures on the potential-energy surface were verified by frequency analysis of the respective optimized geometry. In addition to the sextet spin states given above, also lower multiplicities were considered, but the sextet electromers were energetically the lowest lying throughout at this level of theory. Energies reported here were corrected for zero-point vibrational energy contributions and correspond to free energies at 298.15 K (ΔG_{298}). In the sequence of Figure 3, the corresponding values at 0 K were: 2.34, 1.34, 0.88, and 1.76 eV, respectively, relative to the most stable tautomer $FeCl_2(CH_3OH)^+$.

Acknowledgements

Financial support by the Deutsche Forschungsgemeinschaft, the Sonderforschungsbereich 546, and the Fonds der Chemischen Industrie is gratefully acknowledged. Further, we thank the referees for their helpful and constructive comments.

---

[1] V. E. Bondybey, M. K. Beyer, U. Achatz, B. Fox, G. Niedner-Schatteburg, *Adv. Metal Semicond. Clusters* **2001**, *5*, 295.

[2] P. B. Armentrout, *Int. J. Mass Spectrom.* **2003**, *227*, 289.

[3] J. M. Mercero, J. M. Matxain, X. Lopez, D. M. York, A. Largo, L. A. Eriksson, J. M. Ugalde, *Int. J. Mass Spectrom.* **2005**, *240*, 37.

[4] M. Yamashita, J. B. Fenn, *J. Phys. Chem.* **1984**, *88*, 4451.

[5] M. Yamashita, J. B. Fenn, *J. Phys. Chem.* **1984**, *88*, 4671.

[6] D. A. Plattner, *Int. J. Mass Spectrom.* **2001**, *207*, 125.

[7] J. S. Klassen, Y. Ho, A. T. Blades, P. Kebarle, *Adv. Gas Phase Ion Chem.* **1998**, *3*, 255.

[8] N. G. Tsierkezos, D. Schröder, H. Schwarz, *J. Phys. Chem. A* **2003**, *107*, 9575.

[9] M. Y. Combariza, A. M. Fahey, A. Milshteyn, R. W. Vachet, *Int. J. Mass Spectrom.* **2005**, *244*, 109.

[10] Some reactions of $FeCl_n^+$ ions ($n=0$–2) with isopropanol have been mentioned before without any details being provided, see: D. A. Weil, C. L. Wilkins, *J. Am. Chem. Soc.* **1985**, *107*, 7316.

[11] See also: B. S. Fox, O. P. Balaj, I. Balteanu, M. K. Beyer, V. E. Bondybey, *Chem. Eur. J.* **2002**, *8*, 5534.

[12] These results were obtained by NBO analysis based on DFT calculations; also see Computational Details.

[13] W. A. Brandt, T. Baer, *J. Am. Chem. Soc.* **1984**, *106*, 3154.

[14] C. Lifshitz, *Eur. J. Mass Spectrom.* **2002**, *8*, 85.

[15] D. Schröder, S. Bärsch, H. Schwarz, *J. Phys. Chem. A* **2000**, *104*, 5101.

[16] R. C. Dunbar, *Mass Spectrom. Rev.* **1992**, *11*, 309.

[17] Note that the absence of any signals corresponding to the exchange of [D$_2$]methanol excludes any C-H(D) scrambling being responsible for the observed formation of [D$_1$]- and [D$_3$]methanol; this corroborates the postulated reaction mechanism and rules out C-H(D) bond activation.

[18] In this case, the ^{37}Cl isotopomer was chosen in order to avoid isobaric overlap of $H^{35}Cl$ and CD_3OD formation (both 36 amu).

[19] S. T. Graul, M. D. Brickhouse, R. R. Squires, *J. Am. Chem. Soc.* **1990**, *112*, 631.

[20] As suggested by one referee, it is noted that in case of $n=1$ the large value of x may be explained simply by the occurrence of competing reactions. However, as the trend for the deviation from a collision controlled reaction is distinct also for $n>1$, the x value for $FeCl_2(CH_3OH)^+$ is included into the considerations, as the phenomenon causing the deviations for higher solvated complexes is likely to be operative for $n=1$, too, and thus be at least partially responsible for the deviation of $x=0.61$.

[21] This is only a first-order approximation, because possible isotope effects may slightly change the thermochemistry of ligand exchange.

[22] J. Allison, D. P. Ridge, *J. Am. Chem. Soc.* **1976**, *98*, 7445.

[23] J. Allison, D. P. Ridge, *J. Am. Chem. Soc.* **1979**, *101*, 4998.

[24] K. Eller, W. Zummack, H. Schwarz, *J. Am. Chem. Soc.* **1990**, *112*, 621.

[25] M. J. S. Dewar, *Bull. Soc. Chim. Fr.* **1951**, C71.

[26] J. Chatt, L. A. Duncanson, *J. Chem. Soc.* **1953**, 2939.

[27] a) T. Prüsse, A. Fiedler, H. Schwarz, *J. Am. Chem. Soc.* **1991**, *113*, 8335; b) M. Schlangen, D. Schröder, H. Schwarz, *Helv. Chim. Acta* **2005**, *88*, 1405.

[28] See also: a) C. Trage, W. Zummack, D. Schröder, H. Schwarz, *Angew. Chem.* **2001**, *113*, 2780; *Angew. Chem. Int. Ed.* **2001**, *40*, 2708; b) C. Trage, D. Schröder, H. Schwarz, *Organometallics* **2003**, *22*, 693.

[29] S. G. Lias, J. E. Bartmess, J. F. Liebmann, J. L. Holmes, R. D. Levin, W. G. Mallard, *J. Phys. Chem. Ref. Data* **1988**, *17*, Supplement No 1; URL: http://physics.nist.gov/PhysRefData/.

[30] Also see: D. Schröder, C. Trage, H. Schwarz, D. Danovich, S. Shaik, *Int. J. Mass Spectrom.* **2000**, *200*, 163.

[31] Interestingly, the branching between H_2O and C_3H_6 losses from propanol/$FeCl_2^+$ is opposite to that observed for the system propanol/Fe^+ (see ref. [28]); this fact can be attributed to the different binding energies of iron(I) and iron(III) compounds to σ- and π-donor ligands; also see reference [15].

[32] In consideration of the low intensities of the ions of interest only CID spectra were taken. For cost-efficiency reasons, the spectra were recorded using a solution of $FeCl_3$ (3 mg) in a methanol/water mixture (1:1; 1.25 mL) to which the labeled isopropanol (30 μL) was added. Beforehand, it was ascertained with unlabeled propanol that the Fe(isopropanol)$^+$ ions under investigation remain by and large unaffected upon change of the pure propanol to the methanol/water solvent augmented with as small as possible quantities of isopropanol.

[33] E. P. Hunter, S. G. Lias, *J. Phys. Chem. Ref. Data* **1998**, *27*, 413.

[34] D. Schröder, T. Weiske, H. Schwarz, *Int. J. Mass Spectrom.* **2002**, *219*, 729.

[35] Calculated using the Sheffield Chemputer, see: http://www.shef.ac.uk/chemistry/chemputer (©Mark Winter, University of Sheffield, UK, 1993–2001).

[36] M. Kohler, J. A. Leary, *Int. J. Mass Spectrom. Ion Processes* **1997**, *162*, 17.

[37] D. Schröder, M. Engeser, M. Brönstrup, C. Daniel, J. Spandl, H. Hartl, *Int. J. Mass Spectrom.* **2003**, *228*, 743.

[38] Conversion into absolute rate constants is more difficult to achieve in that the knowledge of the effective length of the hexapole collision cell and thus the effective interaction time as well as the precise kinetic energy distribution is required. As the VG-BIO-Q is not built for such a purpose, both hard- and software restrict kinetic investigations to relative rate constants. However, provided that one of the rates is known from other independent measurements, a conversion to absolute rate constants can be made by calibration.

[39] D. Schröder, M. C. Holthausen, H. Schwarz *J. Phys. Chem. B* **2004**, *108*, 14407.

[40] For details, see: C. Trage, Dissertation, TU Berlin, D83, **2005**.

[41] C. Adamo, V. Barone, *J. Chem. Phys.* **1998**, *108*, 664.

[42] Gaussian 03, Revision C.02, M. J. Frisch, G. W. Trucks, H. B. Schlegel, G. E. Scuseria, M. A. Robb, J. R. Cheeseman, J. A. Montgomery, Jr., T. Vreven, K. N. Kudin, J. C. Burant, J. M. Millam, S. S. Iyengar, J. Tomasi, V. Barone, B. Mennucci, M. Cossi, G. Scalmani, N. Rega, G. A. Petersson, H. Nakatsuji, M. Hada, M. Ehara, K. Toyota, R. Fukuda, J. Hasegawa, M. Ishida, T. Nakajima, Y. Honda, O. Kitao, H. Nakai, M. Klene, X. Li, J. E. Knox, H. P. Hratchian, J. B. Cross, C. Adamo, J. Jaramillo, R. Gomperts, R. E. Stratmann, O. Yazyev, A. J. Austin, R. Cammi, C. Pomelli, J. W. Ochterski, P. Y. Ayala, K. Morokuma, G. A. Voth, P. Salvador, J. J. Dannenberg, V. G. Zakrzewski, S. Dapprich, A. D. Daniels, M. C. Strain, O. Farkas, D. K. Malick, A. D. Rabuck, K. Raghavachari, J. B. Foresman, J. V. Ortiz, Q. Cui, A. G. Baboul, S. Clifford, J. Cioslowski, B. B. Stefanov, G. Liu, A. Liashenko, P. Piskorz, I. Komaromi, R. L. Martin, D. J. Fox, T. Keith, M. A. Al-Laham, C. Y. Peng, A. Nanayakkara, M. Challacombe, P. M. W. Gill, B. Johnson, W. Chen, M. W. Wong, C. Gonzalez, and J. A. Pople, Gaussian, Inc., Wallingford CT, **2004**.

[43] M. Dolg, U. Wedig, H. Stoll, H. Preuss, *J. Chem. Phys.* **1987**, *86*, 866.

Received: June 22, 2005
Revised: October 19, 2005